

## Do spherical $\alpha^2$ -dynamoes oscillate?

G. Rüdiger<sup>1</sup>, D. Elstner<sup>1</sup>, and M. Ossendrijver<sup>2</sup>

<sup>1</sup> Astrophysikalisches Institut Potsdam, An der Sternwarte 16, 14482 Potsdam, Germany

<sup>2</sup> Kiepenheuer-Institut für Sonnenphysik, Schöneckstr. 6, 79104 Freiburg, Germany

Received 9 December 2002 / Accepted 18 April 2003

**Abstract.** The question of whether kinematic  $\alpha^2$ -shell-dynamoes are able to produce a cyclic activity is addressed. The  $\alpha$ -effect is allowed to be latitudinally inhomogeneous and anisotropic but it is assumed as radially uniform in the turbulent shell. For a symmetric  $\alpha$ -tensor we only find oscillatory solutions if i) the  $\alpha$ -tensor component  $\alpha_{zz}$  vanishes or is of the opposite sign as  $\alpha_{\phi\phi}$ , ii) the  $\alpha$ -effect is strongly concentrated in the equatorial region and iii) the  $\alpha$ -effect is concentrated in a rather thin outer shell. In the other cases almost always the nonaxisymmetric field mode S1 (which slowly drifts along the azimuthal direction) possesses the lowest critical dynamo number. The uniform but anisotropic  $\alpha$ -effect (e.g.  $\alpha_{zz} = 0$ ) leads to nonaxisymmetric solutions as is experimentally confirmed by the Karlsruhe dynamo installation.

One of the antisymmetric parts of the  $\alpha$ -tensor, however, plays the role of differential rotation in the induction equation. Using the results of a numerical simulation for the  $\alpha$ -tensor of the solar convection zone for the radial profile of this effect, one finds the possibility of oscillating  $\alpha^2$ -dynamoes even without the existence of a real nonuniform rotation law. Compared with the results of numerical simulations of the full  $\alpha$ -tensor, the amplitude of the antisymmetric part of the tensor must be artificially increased by only a factor of three in order to find oscillating solutions.

**Key words.** magnetohydrodynamics (MHD) – turbulence – stars: activity – earth

### 1. Introduction

There are several observations that in the past have led to increasing interest in the solutions of the relatively simple  $\alpha^2$ -dynamo. The first one is the cyclic orbital modulation of close binary systems such as reported by Hall (1990) and Lanza & Rodonò (1999) for RSCVn stars and the flip-flop phenomenon as reported recently by Tuominen et al. (1999) and Korhonen et al. (2001) for FK Coma stars but also in the single young dwarf LQ Hya (K2V,  $P_{\text{rot}} = 1.6$  days, see Rice & Strassmeier 1998). The fully convective donating stars in short-period cataclysmic variables are suspected to act as  $\alpha^2$ -dynamoes with magnetic poles slowly migrating along the equator (Hessman 2003). Ak et al. (2001) report solar-type cycles for the same class of stars. Together with the highly non-axisymmetric field configurations for very young cool dwarf stars reported by Jardine et al. (2002, see Fig. 1) there is increasing evidence that the traditional stationary and axisymmetric dipole-solution which has been known for decades (see also Charbonneau & MacGregor 2001) is not the final answer. Within the mean-field approximation in turbulent media there are two effects in the equation that generate magnetic flux against the dissipating action of the turbulence. Both effects are linear in the mean magnetic field: the first is the  $\alpha$ -effect and the second is the induction by differential rotation. Only

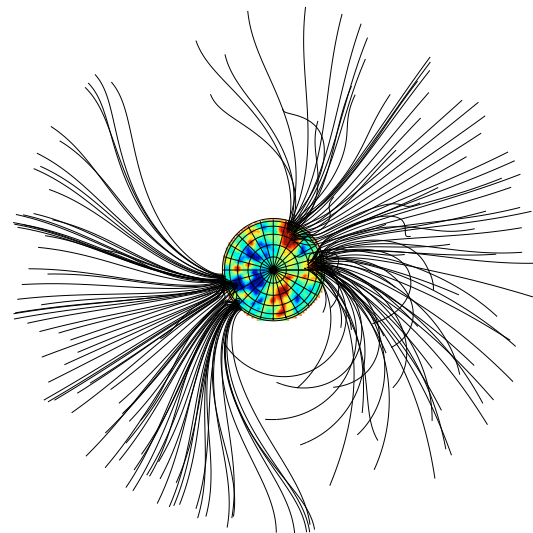


**Fig. 1.** Pole-on representation of the magnetic field of AB Dor. Courtesy M. Jardine.

the internal rotation of the Sun is known, so any *stellar* dynamo model has a rather limited basis. The only exception is the case of rigid rotation which might be realized for fast rotating stars and planets (see Küker & Rüdiger 1999). For such cases it makes sense to consider the simplest magnetic model

Send offprint requests to: G. Rüdiger, e-mail: gruediger@aip.de

for rotating stars with turbulent (outer) convection zones, i.e. the  $\alpha^2$ -dynamo in shells.

The existence of oscillating  $\alpha^2$ -dynamoes was first shown for disk models in local approximation by Shukurov et al. (1985) and Baryshnikova & Shukurov (1987). Rädler & Bräuer (1987) formulated a basic condition for the existence of oscillating modes for mean field dynamoes. They also found that in the local approximation the solutions of the disk dynamo (with constant  $\alpha$  in one hemisphere) never contains the mode with the lowest dynamo number which, however, is a nonoscillating one. So far none of the presented oscillating  $\alpha^2$ -dynamoes proved to be marginal at the dynamo threshold (see, however, our below discussion of the solution of Stefani & Gerbeth). In particular, the inclusion of nonaxisymmetric modes in the calculations was always missing.

In general, however, oscillatory dynamo behavior is produced by a combination of both the  $\alpha$ -effect and differential rotation (“ $\Omega$ -effect”). Kinematic models of the oscillatory solar dynamo were always of the  $\alpha\Omega$ -type. Here, also motivated by the publication of Schubert & Zhang (2000), the question is discussed whether also pure  $\alpha^2$ -dynamoes without any shear flow are able to exhibit oscillatory solutions. Schubert & Zhang considered  $\alpha^2$ -dynamoes with the highly simplifying assumption of a homogeneous and isotropic  $\alpha$ -effect and found oscillatory solutions for thin outer shells similar to the early suggestion of Rädler & Bräuer (1987). In Sect. 3.2 we rediscuss this under the extra condition that only the lowest marginal dynamo number provides a stable solution. If only the lowest dynamo numbers are considered, however, then all solutions for such models will prove to be non-oscillating.

The present paper examines kinematic dynamoes on the basis of  $\alpha$ -tensors derived by the numerical simulations of MHD-convection similar to Ossendrijver et al. (2001, 2002). Nonlinearities in the mean-field dynamo equations are not considered. They are highly complicated as the majority of the resulting kinematic magnetic field configurations is nonaxisymmetric (see Moss & Brandenburg 1995; Küker & Rüdiger 1999).

Within the considered turbulent shell the  $\alpha$ -effect is assumed to be uniform in radius so that there is no change in its sign. Stefani & Gerbeth (2003) have shown that magnetic oscillations can occur if two shells with different signs of the  $\alpha$ -effect exist. The oscillating solution, however, can be shown to disappear for geometries where one sign of the  $\alpha$ -effect dominates the other, as is the case for the simulations shown in Fig. 2. Hence, we do not follow this possibility in the present paper; the  $\alpha$ -effect has here been considered to be uniform in radius within the turbulent shell.

## 2. Basic equations and the model

The model consists of a turbulent fluid in a spherical shell of inner radius  $r_{\text{in}}$  and outer radius  $r_{\text{out}}$ . A magnetic field is generated in the shell by the  $\alpha$ -effect (Steenbeck & Krause 1966; Roberts 1972). In the shell, the turbulent magnetic diffusivity  $\eta_0$  is constant. For  $r > r_{\text{out}}$ , we assume that there is a conductor with large magnetic diffusivity  $\eta_{\text{out}}$ ; for  $r < r_{\text{in}}$ , we assume

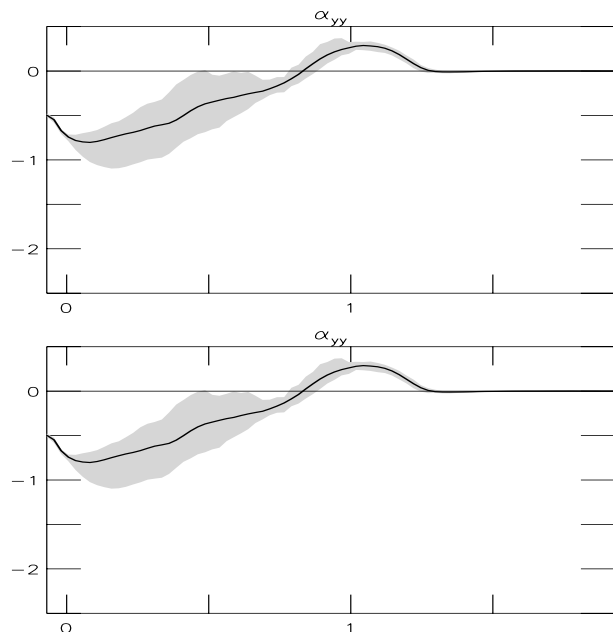


**Fig. 2.** Numerical results for the Cartesian  $\alpha$ -tensor components  $\alpha_{yy} = \alpha_{\phi\phi}$  and  $\alpha_{zz} = \alpha_{rr}$ , measured in units of  $0.01 \sqrt{dg}$ , as a function of depth in units of  $d$  from Ossendrijver et al. (2002) for the case of a box located at the south pole (run A00). The simulation domain consists of a thin cooling layer ( $z < 0$ ), a convectively unstable layer ( $0 < z < d = 1$ ), and a stably stratified layer with overshooting convection ( $z > d$ ). The Coriolis number of the run is about 2.4, which is in the appropriate range for the bottom of the solar convection zone. For the other parameters and for a detailed description of the model we refer to Ossendrijver et al. (2001, 2002). The black curves are spatial and temporal averages; the shaded areas provide an error indication. Note that the  $\alpha_{\phi\phi}$  does not vanish at the pole.

that there is a conductor with high electrical conductivity, i.e. small magnetic diffusivity  $\eta_{\text{in}}$ . The induction equation is

$$\frac{\partial \langle \mathbf{B} \rangle}{\partial t} = \text{curl} \left( \alpha \circ \langle \mathbf{B} \rangle - \eta_{\text{T}} \text{curl} \langle \mathbf{B} \rangle \right), \quad (1)$$

where  $\langle \mathbf{B} \rangle$  is the large-scale magnetic field,  $\eta_{\text{T}}$  is the turbulent magnetic diffusivity and  $\alpha$  is the  $\alpha$ -tensor. For astrophysical applications it represents the interaction of anisotropic turbulence with global rotation and a uniform magnetic field. There are also attempts to include the influence of a nonuniform rotation but this is beyond the scope of the present study. The same holds for the tensorial structure of the eddy diffusivity which indeed exists. As the turbulence is anisotropic, the  $\eta$ -tensor is certainly also anisotropic but the consequences of anisotropic  $\eta$ -tensors for the dynamo solutions seem not to be strong (see Kitchatinov 2002). Note that even the basic effect of topological pumping is part of the  $\alpha$ -tensor which already exists without rotation. Nevertheless, in no known case does the  $\alpha$ -tensor have a simple structure and we are only interested in the structure of the solution of such complicated but pure  $\alpha^2$ -dynamoes.

In Rüdiger & Kitchatinov (1993) one finds the overall structure of the  $\alpha$ -tensor as

$$\alpha_{im} = -\alpha_1 (\mathbf{G}^0 \mathbf{\Omega}^0) \delta_{im} - \alpha_2 (G_i^0 \Omega_m^0 + \Omega_i^0 G_m^0) + \alpha_3 (G_m^0 \Omega_i^0 - G_i^0 \Omega_m^0) - \alpha_4 (\mathbf{G}^0 \mathbf{\Omega}^0) \Omega_i^0 \Omega_m^0 - \gamma \epsilon_{imk} G_k^0. \quad (2)$$

Here the unit vector  $\mathbf{\Omega}^0$  denotes the direction of the axis of the global rotation of the turbulence field and the radial unit vector  $\mathbf{G}^0$  represents its anisotropy. In almost all papers about  $\alpha$ -effect dynamos the expression (2) is reduced to its first term of the tensorial expression. We shall demonstrate, however, that only the inclusion of the remaining parts of the  $\alpha$ -tensor reveals the variety of the solutions of the  $\alpha^2$ -dynamo and also solves the problem of whether  $\alpha^2$ -dynamo can oscillate or not. The influence of any large-scale flow pattern is completely ignored. Then the only remaining dimensionless number is the dynamo number,

$$C_\alpha = \frac{|\alpha_1|R}{\eta_\Gamma}, \quad (3)$$

with  $R$  as the stellar radius.

It is interesting to consider the antisymmetric parts in the tensor (2). A comparison with the induction term  $\mathcal{E}_i = \epsilon_{ikm}u_k B_m$  reveals that the  $\gamma$  in the last term of (2) plays the role of a radial advection (“pumping”) of the magnetic field. On the other hand, if formally a basic rotation with  $\mathbf{u} = \mathbf{\Omega} \times \mathbf{r}$  is used for the velocity field then one obtains  $\mathcal{E}_i = (\mathcal{Q}_m r_i - \mathcal{Q}_i r_m) B_m$ . By comparison with (2) it follows that the  $\alpha_3$ -term in (2) plays the role of global (differential) rotation (see Eq. (9) below). In cylindrical coordinates  $(s, \phi, z)$  we find  $(\alpha_{sz} - \alpha_{zs})/2s$  playing the role of angular velocity, the gradient of which induces magnetic fields. In Sect. 4 we present the influence of the antisymmetric term  $\alpha_3$  in (2) for the existence of oscillating  $\alpha^2$ -dynamo.

An explicit finite difference scheme in two dimensions in spherical coordinates has been used. The standard resolution was  $64 \times 64$  grid points in both radial and latitudinal directions. Some of the calculations were checked with double resolution and/or with a code version in cylindrical coordinates. The models with uniform  $\alpha$ -effect were additionally checked with a spectral method. The values for the minimum dynamo numbers resulted from a global  $\alpha$ -quenching with the total magnetic energy used.

Here and in what follows the fractional radius  $x = r/R$  with  $R$  as the stellar radius is used. The material within the inner boundary is considered as a perfect conductor. The numerical outer boundary of the sphere is fixed at 1.5 stellar radius. Here the standard conditions for a pseudo-vacuum are used. Between  $x = 1$  and  $x = 1.5$  the value for the magnetic diffusivity is increased by a factor 100 in order to mimic vacuum boundary conditions at the stellar surface. In the inner perfect-conducting part ( $x < x_{\text{in}}$ ) the magnetic diffusivity is reduced by a factor of  $10^{-8}$ .

### 3. The symmetric part of the $\alpha$ -tensor

We start in cylindrical coordinates with the symmetric part of the  $\alpha$ -tensor (2), i.e.

$$\alpha \sim \begin{pmatrix} -\alpha_1 \cos \theta & 0 & -\alpha_2 \sin \theta \\ 0 & -\alpha_1 \cos \theta & 0 \\ -\alpha_2 \sin \theta & 0 & -(\alpha_1 + 2\alpha_2 + \alpha_4) \cos \theta \end{pmatrix}. \quad (4)$$

As we shall demonstrate, the ratio

$$\hat{\alpha}_z = \frac{\alpha_1 + 2\alpha_2 + \alpha_4}{\alpha_1} \quad (5)$$

will be of particular relevance for the resulting solutions. In spherical coordinates  $(r, \theta, \phi)$  we have the general structure

$$\alpha \sim \begin{pmatrix} \alpha_{rr} & \alpha_{r\theta} & 0 \\ \alpha_{\theta r} & \alpha_{\theta\theta} & 0 \\ 0 & 0 & \alpha_{\phi\phi} \end{pmatrix} \quad (6)$$

with  $\alpha_{rr} = -(\alpha_1 + 2\alpha_2 + \alpha_4 \cos^2 \theta) \cos \theta$ ,  $\alpha_{r\theta} = \alpha_{\theta r} = (\alpha_2 + \alpha_4 \cos^2 \theta) \sin \theta$ ,  $\alpha_{\theta\theta} = -(\alpha_1 + \alpha_4 \sin^2 \theta) \cos \theta$  and  $\alpha_{\phi\phi} = -\alpha_1 \cos \theta$  so that for the ratio (5) the expression

$$\hat{\alpha}_z = \frac{\alpha_{rr}(\text{pole})}{\alpha_{\phi\phi}(\text{pole})} \quad (7)$$

results where any of the two poles can be taken.

#### 3.1. The $\alpha$ -tensor elements

Ossendrijver et al. (2001, 2002) present simulations for all the components of the  $\alpha$ -tensor in spherical coordinates. Some of the results, which are relevant for the present discussion, are reported here. The simulations were done in a Cartesian box which is meant to represent a section from the lower part of a stellar convection zone, including a convectively stable layer underneath it. The Cartesian coordinate frame of the box corresponds to the spherical coordinates introduced above, such that the  $x$ -direction corresponds to the negative  $\theta$ -direction, the  $y$ -direction to the  $\phi$ -direction, and the  $z$ -direction (depth) to the negative  $r$ -direction. All simulations were done at the southern hemisphere of the star, and the angle between the vertical (radial) direction and the axis of rotation was varied between  $0^\circ$  (south pole) and  $90^\circ$  (equator). Provided the rotation rate is sufficient to yield an  $\alpha$ -effect, the depth dependence of  $\alpha_{\theta\theta}$  and  $\alpha_{\phi\phi}$  has a typical shape, namely a negative sign in the bulk of the convection zone and a positive sign in the thin overshooting layer. These features are expected for the southern hemisphere. The amplitudes of  $\alpha_{\theta\theta}$  and  $\alpha_{\phi\phi}$  increase with increasing angular distance from the equator up to a point close to the south pole, more or less consistent with the commonly assumed  $\cos \theta$ -function. Hence, the  $\alpha$ -effect does *not* vanish at the poles. For weak rotation, the component  $\alpha_{rr}$  has a larger amplitude than the other two diagonal components, and it has the *opposite sign*. If rotation increases beyond a certain point,  $\alpha_{rr}$  as a function of depth develops multiple sign changes, unlike  $\alpha_{\theta\theta}$  and  $\alpha_{\phi\phi}$ , and its amplitude falls behind that of the latter. This is the rotational quenching of the vertical alpha effect reported in Ossendrijver et al. (2001). In the overshoot region, after (7) the  $\hat{\alpha}_z$  is still negative so that again the  $\alpha_{zz}$ -component of the tensor (in cylindrical coordinates) has the opposite sign as  $\alpha_{\phi\phi}$  (Rüdiger 1980).

The symmetric component  $\alpha_{r\theta}^S = \alpha_{z\phi}^S$  is positive in the bulk of the unstable layer, and is generally larger in magnitude than  $\alpha_{r\theta}^A$ ; it vanishes at the poles.

#### 3.2. Dynamos for homogeneous $\alpha$ -effect

There are references in the literature where the basic antisymmetry of the  $\alpha$ -effect with respect to the equatorial midplane has been neglected (Rädler & Bräuer 1987;

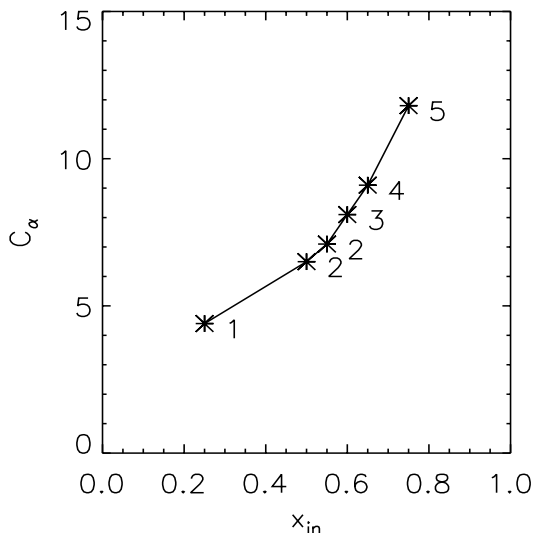


**Fig. 3.** Homogeneous and isotropic  $\alpha$ -effect: the lowest critical dynamo numbers  $C_\alpha$  for models with various positions  $x_i$  of the shell bottom. All the solutions are non-oscillating. The curve is marked with the latitudinal mode number  $n$  for which the dynamo number is minimum. The  $C_\alpha$  for the oscillating modes found by Schubert & Zhang (2000) are always located *above* this line.

Schubert & Zhang 2000; Stefani & Gerbeth 2000; Rädler et al. 2002). The realization of such models can only be imagined in technical installations. Indeed, the paper by Rädler et al. (2002) concerns the Karlsruhe dynamo experiment with a fixed helicity and a uniform flow field in vertical ( $z$ -)direction of a cylindrical coordinate system, so that  $\alpha_{zz} = 0$  is obvious. In order to demonstrate the differences between isotropic and anisotropic  $\alpha$ -tensors also in the case of homogeneous  $\alpha$ -effect (i.e.  $\cos \theta$  ignored), the following calculations are presented for the cases i)  $\alpha_{zz} = \alpha_{\phi\phi}$ , i.e.  $\hat{\alpha}_z = 1$  and ii)  $\alpha_{zz} = 0$ , i.e.  $\hat{\alpha}_z = 0$ . While the first case seems to be an often discussed but academic problem, the second one fits the situation in the dynamo experiment mentioned.

We start with spherical models with outer  $\alpha$ -effect zone located between  $x = x_{in}$  and  $x = 1$  and embedded in a vacuum<sup>1</sup>. In this zone, the  $\alpha$ -effect and eddy diffusivity  $\eta_T$  are assumed as radially uniform, but below the convection zone there is a steep transition zone to the perfect-conducting interior with a magnetic diffusivity reduced by a factor of 100. Always the modes with the lowest dynamo numbers  $C_\alpha$  are considered in the present paper. Each mode has its own dynamo number; the mode with the lowest dynamo number is the preferred stable mode (Krause & Meinel 1988).

The problem of both homogeneous *and* isotropic  $\alpha$ -effect (i.e.  $\alpha_{im} = \alpha_0 \delta_{im}$  with  $\alpha_0 = \text{const.}$ ) has been considered by Schubert & Zhang (2000). Our results do not agree with theirs if indeed only the solutions with the *lowest* dynamo numbers are considered. In Fig. 3 the resulting minimum dynamo numbers  $C_\alpha$  and the associated latitudinal mode numbers  $n$  are given for various inner shell radii  $x_{in}$ . In opposition to the case

<sup>1</sup> Test computations for models embedded in a perfect conductor did not reveal basic modifications of our results, in contrast to the remark by Brandenburg (1994).

**Table 1.** Marginal dynamo numbers for axisymmetric and nonaxisymmetric magnetic field modes for anisotropic ( $\alpha_{zz} = 0$ ) but uniform  $\alpha$ -effect ( $\alpha = \text{const.}$ , cf. Karlsruhe dynamo experiment). The boldface numbers mark the magnetic mode with the lowest dynamo number.

| $x_{in}$ | A0          | S0          | A1           | S1           |
|----------|-------------|-------------|--------------|--------------|
| 0.25     | 9.06        | 8.40        | <b>6.72</b>  | <b>6.72</b>  |
| 0.50     | 10.84 (osc) | 10.64 (osc) | <b>9.50</b>  | <b>9.50</b>  |
| 0.75     | 17.29 (osc) | 17.32 (osc) | <b>16.23</b> | <b>16.23</b> |

**Table 2.** The same as in Table 1 but for  $\alpha \sim \cos \theta$ .

| $x_{in}$ | A0          | S0          | A1           | S1           |
|----------|-------------|-------------|--------------|--------------|
| 0.25     | 14.99 (osc) | 14.94 (osc) | 10.64        | <b>9.97</b>  |
| 0.50     | 15.7 (osc)  | 15.5 (osc)  | 11.8         | <b>11.7</b>  |
| 0.75     | 21.58 (osc) | 21.58 (osc) | <b>18.43</b> | <b>18.43</b> |

of latitudinally inhomogeneous  $\alpha$ -effect ( $\sim \cos \theta$ ) the solutions of the induction Eq. (1) are modes with a single latitudinal mode number  $n$ . All the solutions can thus be characterized by the mode number  $n$ ; the solutions with the mode number  $n$  and with the lowest value of  $C_\alpha$  are given in Fig. 3 – they all are non-oscillating. We do not find any oscillating  $\alpha^2$ -dynamo unless its  $\alpha$ -amplitude was not the lowest one. As we see in Fig. 3, however, it is clear that it is *not* enough to consider only the modes with  $n = 1$  or  $n = 2$ . The thinner the (outer)  $\alpha$ -shell, the higher is the latitudinal mode number  $n$  of the modes excited with the lowest dynamo number  $C_\alpha$ . Oscillating modes with low  $n$  also exist but for thin shells their  $C_\alpha$  is never the lowest one. The same remark concerns the analysis of Rädler & Bräuer (1987).

More interesting are the solutions with homogeneous but anisotropic  $\alpha$ -tensors. The  $\alpha$ -tensor has no  $zz$ -component, i.e.  $\alpha_{zz} = 0$  in cylindrical coordinates. Now the rotation axis is clearly defined so that it makes sense to look for the axisymmetry of the solutions. Table 1 gives the results for a uniform  $\alpha$ -effect and Table 2 gives the results if the  $\alpha$ -effect is antisymmetric with respect to the equator, i.e.  $\alpha \sim \cos \theta$ . Our notation is the standard one, i.e.  $Am$  denotes a solution with antisymmetry with respect to the equator and with the azimuthal quantum number  $m$  while  $Sm$  denotes a solution with symmetry with respect to the equator (see Krause & Rädler 1980). The oscillating solar magnetic field mode is antisymmetric with respect to the equator, it is of A0 type. It was important to include the nonaxisymmetric modes in the consideration as they possess the lowest dynamo numbers. The nonaxisymmetric modes with  $m = 1$  always dominate for all the models considered; there are no oscillations. The axisymmetric solutions (mostly oscillating) that have been found by Busse & Miin (1979), Weisshaar (1982) and Olson & Hagee (1990) are probably not stable as the solution with the lowest dynamo number is nonaxisymmetric and azimuthally drifting rather than axisymmetric and oscillating.

There are no basic differences for the cases in Tables 1 and 2, i.e. for  $\alpha \sim \text{const.}$  and  $\alpha \sim \cos \theta$  ( $\alpha_{zz} = 0$  in both cases).

**Table 3.** Dynamo numbers  $C_\alpha$  for isotropic  $\alpha$ -effect ( $\hat{\alpha}_z = 1$ ). The bottom of the convection zone is at  $x_{\text{in}} = 0.5$ . The boldface numbers mark the lowest value of the dynamo number.

| $\lambda$ | A0          | S0         | A1          | S1          |
|-----------|-------------|------------|-------------|-------------|
| 0         | <b>9.41</b> | 9.42       | 9.75        | 9.76        |
| 1         | 28.8 (osc)  | 28.7 (osc) | <b>26.7</b> | <b>26.7</b> |
| 2         | 41.1 (osc)  | 41.2 (osc) | <b>38.8</b> | 39.2        |
| 3         | 51.9 (osc)  | 52.0 (osc) | <b>49.8</b> | 50.3        |

**Table 4.** The same as in Table 3 but for  $\hat{\alpha}_z = 0$ .

| $\lambda$ | A0         | S0         | A1   | S1          |
|-----------|------------|------------|------|-------------|
| 0         | 15.7 (osc) | 15.5 (osc) | 11.8 | <b>11.7</b> |
| 1         | 35.0 (osc) | 33.8 (osc) | 32.7 | <b>31.3</b> |
| 2         | 51.7 (osc) | 49.1 (osc) | 49.3 | <b>47.0</b> |
| 3         | 66.6 (osc) | 63.3 (osc) | 64.3 | <b>61.4</b> |

The exceptional role of the modes with  $m = 1$  for an anisotropic  $\alpha$ -effect is a well-known result that has already been presented by Rüdiger (1980) and by Rüdiger & Elstner (1994). Here we have added its relevance also for the more simple case of a *homogeneous*  $\alpha$ -effect. In the light of these calculations it is thus not a surprise that the Karlsruhe dynamo experiment provides the nonaxisymmetric modes with  $m = 1$  (Stieglitz & Müller 2001).

### 3.3. Dynamoes for an inhomogeneous $\alpha$ -effect

In the following we shall develop further the models with equatorial antisymmetry of the  $\alpha$ -effect as a consequence of a global rotation of the considered sphere. We apply different  $\alpha$ -profiles in latitude in order to simulate a possible concentration of the  $\alpha$ -effect around the equator. We fix the latitudinal profile as

$$\alpha \propto \sin^{2\lambda} \theta \cos \theta, \quad (8)$$

where  $\lambda$  is a free parameter describing the latitudinal profile of the  $\alpha$ -effect. For  $\lambda > 0$  the  $\alpha$ -effect at the poles vanishes. For increasing values of  $\lambda$  it is more and more concentrated at lower latitudes. Note, however, that the box simulations did not reveal deviations of the latitudinal  $\alpha$ -profile from the  $\cos \theta$ -law with  $\lambda = 0$  (Ossendrijver et al. 2001). In particular, at the poles the effect did *not* vanish. Thus, the dynamo models with  $\lambda > 0$  seem to be only of academic interest, but it is necessary to know that only for such models do oscillating solutions appear with the lowest dynamo numbers.

The results for kinematic dynamo models with (realistic) equatorial antisymmetry are summarized in Tables 3–5 presenting the critical  $C_\alpha$  for different  $\alpha$ -tensor models and convection zones with various depths.

Table 3 gives the results for an *isotropic*  $\alpha$ -effect ( $\hat{\alpha}_z = 1$ ). The boldface numbers represent the absolutely lowest  $C_\alpha$  indicating stability. For the standard case with  $\lambda = 0$ , Table 3 provides the axisymmetric dipole A0 as the stable mode. This

**Table 5.** The same as in Table 4 but for  $x_{\text{in}} = 0.8$ .

| $\lambda$ | A0          | S0                 | A1          | S1          |
|-----------|-------------|--------------------|-------------|-------------|
| 0         | 26.3 (osc)  | 26.3 (osc)         | <b>23.2</b> | <b>23.2</b> |
| 1         | 63.0 (osc)  | <b>62.9</b> (osc)  | 63.0        | <b>62.9</b> |
| 2         | 89.8 (osc)  | <b>89.4</b> (osc)  | 90.2        | 89.9        |
| 3         | 112.9 (osc) | <b>111.8</b> (osc) | 113.4       | 112.7       |

result, however, strongly depends on the latitudinal profile of the  $\alpha$ -effect. Already for  $\lambda = 1$  the preferred mode is non-axisymmetric, i.e. A1 and/or S1 and for  $\lambda = 2$  and 3 we always find the A1 mode as the preferred one. Our result is that except for the simplest latitudinal profile of the  $\alpha$ -effect (i.e. the  $\cos \theta$ -dependence), the solutions are no longer axisymmetric, so that the work with codes for two-dimensional (axisymmetric) magnetic field configurations only has a very restricted meaning. Although oscillating modes also appear, they never have the lowest dynamo numbers. Note that from all our latitudinal  $\alpha$ -profiles only the  $\cos \theta$ -dependence leads to nonvanishing  $\alpha$ -values at the poles.

For the anisotropic  $\alpha$ -tensor we have a clearer situation. Simplifying, we worked with  $\hat{\alpha}_z = 0$ . The Table 4 presents the results. The preferred solutions are always nonaxisymmetric since the oscillating axisymmetric modes always possess higher  $C_\alpha$  values. Oscillating axisymmetric solutions occur, however, for the same  $\alpha$ -anisotropy but for thin convection zones with  $x_{\text{in}} = 0.8$  and  $\lambda > 0$  (Table 5). For such a model where the  $\alpha$ -effect does *not* exist in the polar regions we find that the mode with the lowest  $C_\alpha$  (i.e. the stable mode) forms oscillating axisymmetric magnetic fields (of quadrupolar equatorial symmetry, no dipoles). However, such a cyclic behavior seems to be a rather exceptional case as it only appears if three conditions are fulfilled, i.e.

- i) the  $\alpha$ -tensor must be highly anisotropic,
- ii) the  $\alpha$ -effect must be concentrated to the equator,
- iii) the convection zone must be rather thin.

The latter condition resembles a similar finding of Rädler & Bräuer (1987) – but in contrast to their consideration the thin-shell condition is *not* sufficient for oscillating  $\alpha^2$ -dynamoes.

## 4. The antisymmetric part of the $\alpha$ -tensor

Let us now turn to the antisymmetric parts of the  $\alpha$ -tensor. There is at first the  $\alpha_3$ -component in the tensor formulation (2). As mentioned above, it formally acts as (differential) rotation – so that in reality, if  $\alpha_3$  is not too small – *all*  $\alpha^2$ -dynamoes can operate as (pseudo)  $\alpha\Omega$ -dynamoes which finally are known as oscillatory. We shall denote this virtual angular velocity by  $\Omega_T$  with

$$\Omega_T = -\frac{\alpha_3}{x}. \quad (9)$$

Obviously, the ratio  $\alpha_3/\alpha_1$  will determine the ability of the  $\alpha^2$ -dynamo to operate as a (pseudo)  $\alpha\Omega$ -dynamo. In any case,

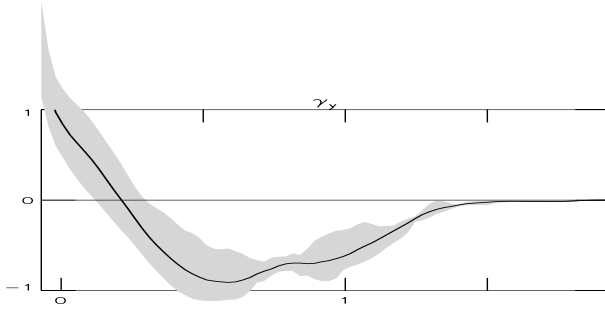


**Fig. 4.** Pumping velocity  $\gamma_\phi = \gamma_y$ , measured in units of  $0.01 \sqrt{dg}$ , as a function of depth in units of  $d$  from Ossendrijver et al. (2002) for the case of a box located at the equator (their Fig. 4). The tensor quantity  $\gamma_\phi$  equals  $x\Omega_T$ .

however, it transforms poloidal magnetic fields to toroidal magnetic fields with a phase relation depending on the sign of  $\partial\Omega_T/\partial r^2$ .

In spherical coordinates the antisymmetric parts of the  $\alpha$ -tensor (2) can be written as

$$\alpha \sim \begin{pmatrix} 0 & \sin\theta \alpha_3 & 0 \\ -\sin\theta \alpha_3 & 0 & -\gamma \\ 0 & \gamma & 0 \end{pmatrix}. \quad (10)$$

With the notation in Ossendrijver et al. (2002)  $\alpha_3 = -\gamma_\phi / \sin\theta$ , i.e.  $\alpha_3 = -\gamma_\phi$  (equator) is found.

#### 4.1. Simulations

From Ossendrijver et al. (2002) the following numerical results on  $\gamma_r$  and  $\gamma_\phi$  can be summarized. The longitudinal pumping ( $\gamma_\phi$ ) is generally the strongest pumping effect observed in the simulations in the equatorial region. It has a predominantly negative sign within the bulk of the unstable layer and in the overshoot layer, which signifies that the mean field is advected in the retrograde direction (see Fig. 4). In most cases reported in Ossendrijver et al. (2002) there is also a thin layer near the top of the convection zone where the field is pumped in the prograde direction. The longitudinal pumping effect is strongly dependent on latitude; it vanishes at the pole and peaks at the equator.

The direction of vertical pumping ( $\gamma_r$ ) is downward ( $\gamma_r < 0$ ) in the bulk of the unstable layer and in the overshoot layer. Only near the top of the box is there a thin layer where the pumping is directed upwards ( $\gamma_r > 0$ ). There is only little dependence on latitude or rotation.

#### 4.2. Results

We start with the (unrealistic) case of radially uniform  $\alpha_3$  where it is measured in units of  $|\alpha_1|$ , i.e.  $\hat{\alpha}_3 = \alpha_3/|\alpha_1|$ . Then after (9) it is  $\partial\Omega_T/\partial x = \alpha_3/x^2$  so that it mimics superrotation for positive  $\alpha_3$ . Characteristic results are given in Table 6. For too small  $\alpha_3$ , the nonaxisymmetric solution (S1) of the  $\alpha^2$ -dynamo is hardly influenced. For  $\hat{\alpha}_3 \approx 10$ , however, we already find an oscillating quadrupole. Between  $\hat{\alpha}_3 = 5$  and  $\hat{\alpha}_3 = 10$  the

<sup>2</sup>  $\text{sign}(B_r B_\phi) = \text{sign}(\partial\Omega_T/\partial r)$ .

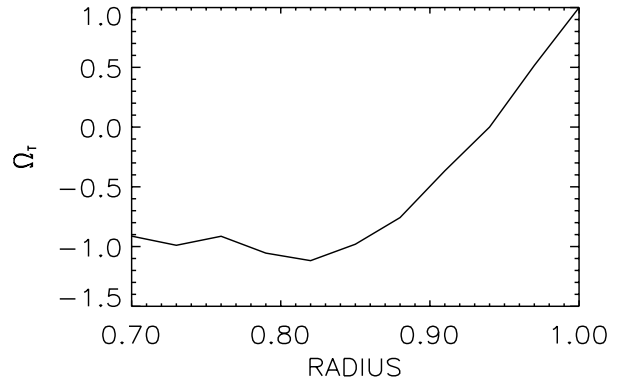


**Fig. 5.** The same as in Fig. 4 but in the representation  $\Omega_T = \Omega_T(x)$  (see Eq. (9)).

**Table 6.** Dynamo numbers for anisotropic  $\alpha$ -effect with  $\hat{\alpha}_z = 0$  and uniform  $\alpha_3$ -effect.  $x_{\text{in}} = 0.5$ ,  $\alpha_2 = 0$ .

| $\hat{\alpha}_3$ | A0         | S0                | A1   | S1          |
|------------------|------------|-------------------|------|-------------|
| 3                | 14.9 (osc) | 14.4 (osc)        | 12.1 | <b>12.0</b> |
| 5                | 14.3 (osc) | 13.7 (osc)        | 12.9 | <b>12.9</b> |
| 10               | 12.9 (osc) | <b>12.0</b> (osc) | 15.0 | 15.1        |

**Table 7.** Dynamo numbers for anisotropic  $\alpha$  ( $\hat{\alpha}_z = 0$ ) and nonuniform  $\alpha_3$ -effect (see Figs. 4 and 5).  $x_{\text{in}} = 0.5$ ,  $\alpha_2 = 0$ .

| $\hat{\alpha}_3$ | A0                | S0                | A1   | S1          |
|------------------|-------------------|-------------------|------|-------------|
| 1                | 15.1 (osc)        | 14.8 (osc)        | 12.1 | <b>11.9</b> |
| 2                | 14.9 (osc)        | 14.5 (osc)        | 12.9 | <b>12.8</b> |
| 3                | 15.0 (osc)        | <b>14.6</b> (osc) | 17.4 | 17.4        |
| -10              | <b>14.7</b> (osc) | <b>14.7</b> (osc) | 16.6 | 16.6        |

transition occurs from nonaxisymmetric drifting modes to axisymmetric oscillating solutions.

Obviously, the considered values of  $\alpha_3$  for the transition to a pseudo  $\alpha\Omega$ -dynamo are rather high. It is the non-uniformity of the  $\Omega_T$ -effect that appears in the induction equation and may allow the oscillations. We have thus applied the radial profile in Fig. 5 to the model which results from real simulations (Ossendrijver et al. 2002). The profile is multiplied by the amplitude  $\hat{\alpha}_3$  which is varied in order to find the various dynamo solutions. The results are given in Table 7 and they are a surprise. Indeed, the amplification of the  $\alpha_3$ -effect by only a factor of 3 leads to the appearance of oscillating solutions as the most stable. Again it shows quadrupolar symmetry. Dipolar symmetry only appears for the amplification factor of  $\hat{\alpha}_3 = -10$ . Hence, the  $\alpha\Omega_T$ -dynamo resulting from the simulations of Ossendrijver et al. may easily lead to oscillating solutions, here in our models with quadrupolar symmetry.

## 5. Discussion

We have shown that for spherical configurations with outer turbulent shells the basic solution for  $\alpha^2$ -dynamoes is a nonaxisymmetric mode drifting in the azimuthal direction. Oscillating axisymmetric solutions are seldom exceptions for  $\alpha$ -effects that are

- i) highly anisotropic,
- ii) strongly concentrated to the equatorial region,
- iii) restricted to thin outer shells.

In all other cases the mode with the lowest  $C_\alpha$  (which are considered here as the only stable one) is nonaxisymmetric and almost always of quadrupolar symmetry. The azimuthal drift is always of the same order as the oscillation frequencies. Note that the box simulations by Ossendrijver et al. (2001) did *not* lead to a vanishing  $\alpha$ -effect at the poles.

The same is true for  $\alpha^2$ -dynamoes under inclusion of those anisotropic parts of the  $\alpha$ -tensor that can be combined with antisymmetric components, i.e.  $G_i\Omega_m - G_m\Omega_i$ . This term corresponds to a (pseudo-)angular velocity  $\Omega_T$  (see Eq. (9)) which induces electrical fields in the same way as a real differential rotation of the plasma would do. The box simulations of Ossendrijver et al. reveal this  $\Omega_T$  as increasing outwards (see Fig. 5) so that in any case, together with the positive  $\alpha_{\phi\phi}$  (in the northern hemisphere), an antisolar butterfly diagram results if the solution is axisymmetric and oscillating. To this end the amplitude of the  $\alpha_3$ -effect must be artificially increased by a (small) factor of 3. Oscillating dipolar solutions only exist if the  $\Omega_T$ -effect is artificially amplified by a factor of minus 10 (see Table 7).

We conclude that shell-dynamoes on the basis of MHD simulations of rotating stellar convection without real differential rotation always possess nonaxisymmetric magnetic field configurations such as recently found for AB Dor. Oscillating solutions for  $\alpha^2$ -dynamoes are revealed as exotic exceptions. Our conclusion is that a cyclic stellar activity can thus always be considered as a strong indication of the existence of real internal differential rotation.

## References

- Ak, T., Ozkan, T., & Mattei, J. A. 2001, *A&A*, 369, 888  
 Baryshnikova, Y., & Shukurov, A. 1987, *Astron. Nachr.*, 308, 89  
 Brandenburg, A. 1994, Solar dynamoes: Computational background, in *Lectures on Solar and Planetary Dynamoes*, ed. M. R. E. Proctor, & A. D. Gilbert (Cambridge University Press), 117  
 Busse, F. H., & Miin, S. W. 1979, *Geophys. Astrophys. Fluid Dyn.*, 14, 167  
 Charbonneau, P., & MacGregor, K. B. 2001, *ApJ*, 559, 1094  
 Hall, D. S. 1990, Period changes and magnetic cycles, in *Active close binaries*, ed. C. Ibanoglu (Dordrecht: Kluwer Academic), 95  
 Hessman, F. V. 2003, Dynamo-induced mass-transfer variations in MCV's, in *Magnetic Cataclysmic Variables*, IAU 190  
 Jardine, M., Collier Cameron, A., & Donati, J.-F. 2002, *MNRAS*, 333, 339  
 Kitchatinov, L. L. 2002, *A&A*, 394, 1135  
 Korhonen, H., Berdyugina, S. V., Strassmeier, K. G., & Tuominen, I. 2001, *A&A*, 379, L30  
 Krause, F., & Meinel, R. 1988, *Geophys. Astrophys. Fluid Dyn.*, 43, 95  
 Krause, F., & Rädler, K.-H. 1980, *Mean-field magnetohydrodynamics and dynamo theory* (Oxford: Pergamon Press)  
 Küker, M., & Rüdiger, G. 1999, *A&A*, 346, 922  
 Lanza, A. F., & Rodonò, M. 1999, *A&A*, 349, 887  
 Moss, D., & Brandenburg, A. 1995, *Geophys. Astrophys. Fluid Dyn.*, 80, 229  
 Olson, P., & Hagee, V. L. 1990, *J. Geophys. Res.*, 95, 4609  
 Ossendrijver, M., Stix, M., & Brandenburg, A. 2001, *A&A*, 376, 713  
 Ossendrijver, M., Stix, M., Brandenburg, A., & Rüdiger, G. 2002, *A&A*, 394, 735  
 Rädler, K.-H., & Bräuer, H.-J. 1987, *Astron. Nachr.*, 308, 101  
 Rädler, K.-H., Rheinhardt, M., Apstein, E., & Fuchs, H. 2002, *Nonlinear Processes in Geophysics*, 9, 171  
 Rice, J. B., & Strassmeier, K. G. 1998, *A&A*, 336, 972  
 Roberts, P. H. 1972, *Phil. Trans. R. Soc. London A*, 272, 663  
 Rüdiger, G. 1980, *Astron. Nachr.*, 301, 181  
 Rüdiger, G., & Elstner, D. 1994, *A&A*, 281, 46  
 Rüdiger, G., & Kitchatinov, L. L. 1993, *A&A*, 269, 581  
 Schubert, G., & Zhang, K. 2000, *ApJ*, 532, 149  
 Shukurov, A. M., Sokolov, D. D., & Ruzmaikin, A. A. 1985, *Magnetohydrodynamics*, 21, 6  
 Steenbeck, M., & Krause, F. 1966, *Z. Naturforsch. A*, 21, 1285  
 Stefani F., & Gerbeth, G. 2000, *Astron. Nachr.*, 321, 235  
 Stefani F., & Gerbeth, G. 2003, *Phys. Rev. E*, 67, 027302  
 Stieglitz, R., & Müller, U. 2001, *Phys. Fluids*, 13, 561  
 Tuominen, I., Berdyugina, S. V., Korpi, M. J., & Rönty, T. 1999, Nonaxisymmetric stellar dynamoes, in *Stellar dynamoes: Nonlinearity and chaotic flows*, ed. M. Nunez, & A. Ferriz-Mas, *ASP Conf. Ser.*, 178, 195  
 Weisshaar, E. 1982, *Geophys. Astrophys. Fluid Dyn.*, 21, 285